Analysis of recent VLBI catalogs

Sébastien B. Lambert

SYRTE, Observatoire de Paris, PSL Research University, CNRS, Sorbonne Universités, UPMC Univ. Paris 06, LNE
61 av. de l'Observatoire, 75014 Paris, France
Phone: +33 1 40 51 22 33
E-mail: sebastien.lambert@obspm.fr

1. Data sets

Six catalogs were submitted respectively by the Italian Space Agency (ASI; asi2016a), Geoscience Australia (aus2016a; aus201b), the Federal Agency for Cartography and Geodesy (BKG Leipzig) and Institute of Geodesy and Geoinformation of the University of Bonn (IGGB; bkg2016a), and the US Naval Observatory (usn2016a). All these catalogs provide right ascension (α) and declination (δ) of extragalactic radio sources, as well as their respective uncertainties, the correlation coefficient between α and δ, and the number of sessions and delays. Note that bkg2016a and usn2016a catalogs were produced with the same geodetic VLBI analysis software package SOLVE developed at NASA GSFC. Solutions aus2016a and aus2016b were produced with OCCAM. The catalogs are displayed in Fig. 1 with color codes following the formal error on the source position.

Table 1 displays the total number of sources of each catalog, as well as the number of sources in common with the ICRF2 (Fey et al. 2015) and the Gaia DR1 auxiliary solution (Mignard et al. 2016). Table 1 also reports the median error and reveals an error in declination larger than in right ascension by a factor of ~1.5. The error is substantially smaller for SOLVE solutions compared to OCCAM, except the solution asi2016a whose smaller error likely originates in the fact that the solution considered a relatively small number of well observed sources with low positional standard error.

Table 1. Number of sources (total and in common with ICRF2 and the Gaia DR1 catalog) and median error (in microarc second). Values for right ascension, referred to as RA*, are corrected from the cosine of the declination.

	No Sources			Median Err	
	Total	ICRF2	Gaia	RA*	Dec
asi2016a	1368	1339	958	56	92
aus2016a	3900	3284	2106	442	728
aus2016b	3917	3290	2109	432	700
bkg2016a	3507	3122	2029	234	428
usn2016a	4129	3412	2191	213	364

Figure 2 illustrates how the overall formal error, defined as the square root of $\sigma_{\alpha\cos\delta}^2 + \sigma_\delta^2 + c\sigma_{\alpha\cos\delta}\sigma_{\alpha\delta}$ where σ is the formal error listed in the catalogs and c is the correlation coefficient between estimates of α and δ as provided in the catalogs, varies with the number N of observations. The figure for aus2016b clearly shows that some sources have underestimated formal errors likely due to an overconstrained solution. (As stated in the technical document delivered with the catalog, a strong no-net rotation condition was imposed to these sources. A similar fact was pointed for solution aus2015a in the 2014 IERS Annual Report.) The formal error of the same sources in solution aus2016a, in which the no-net rotation condition is less severe, appears to be at a level comparable to other sources.
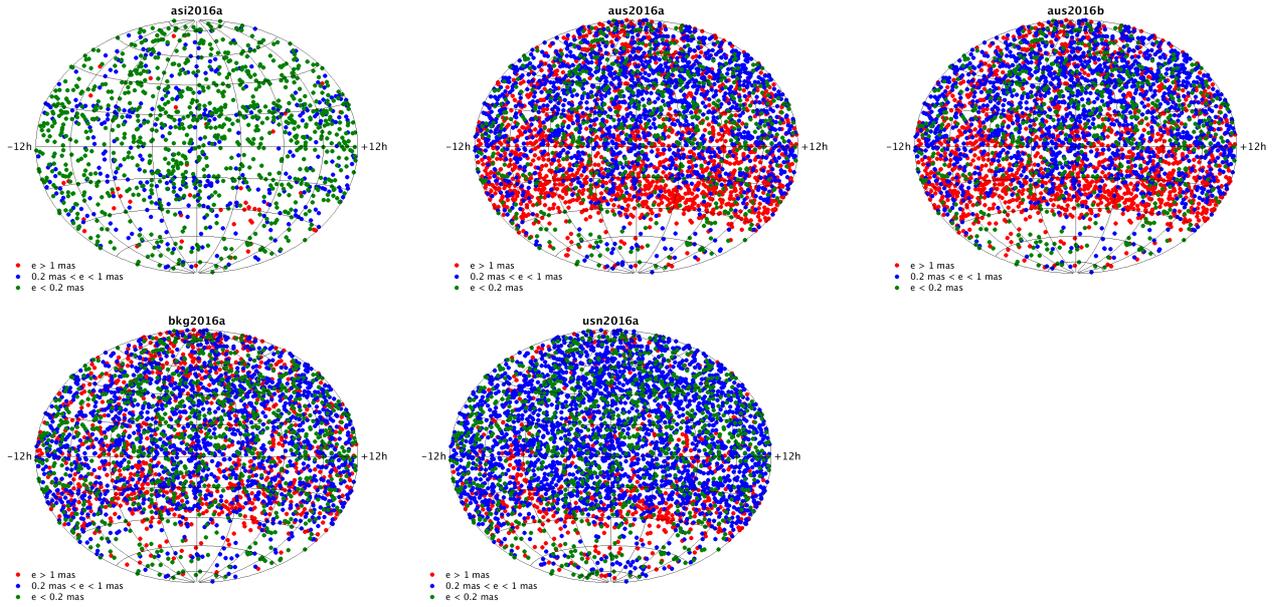
Figure 1. The source distribution on the sky.
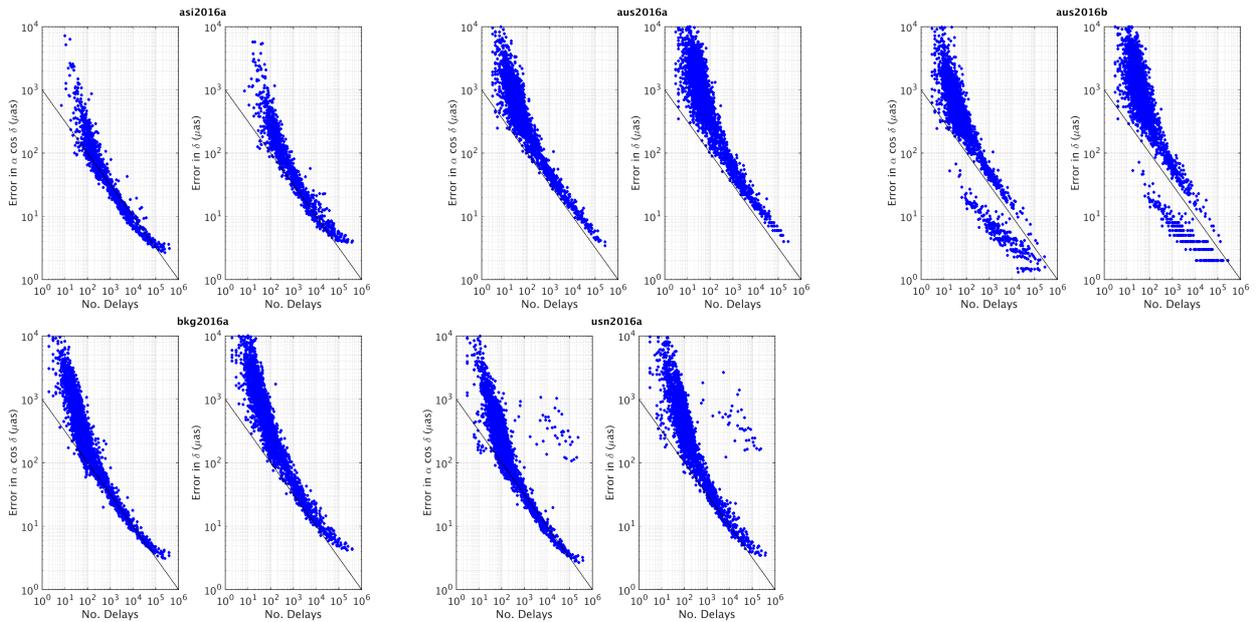
Figure 2. The formal error as a function of the number of delays. See text for details.

2. Frame deformation

We evaluate the consistency of the submitted catalogs with the ICRF2 and Gaia DR1 by modeling the coordinate difference (in the sense catalog minus reference) by a 16-parameter transformation including three rotations, a glide (three parameters), and a quadrupolar deformation (e.g., Mignard and Klioner 2012).

$$
\begin{aligned}
\Delta\alpha\cos\delta \;=\;& R_1\cos\alpha\sin\delta + R_2\sin\alpha\sin\delta - R_3\cos\delta - D_1\sin\alpha + D_2\cos\alpha + a_{20}^{M}\sin 2\delta \\
+\;& \left(a_{21}^{E,\mathrm{Re}}\sin\alpha + a_{21}^{E,\mathrm{Im}}\cos\alpha\right)\sin\delta - \left(a_{21}^{M,\mathrm{Re}}\cos\alpha - a_{21}^{M,\mathrm{Im}}\sin\alpha\right)\cos 2\delta \\
-\;& 2\left(a_{22}^{E,\mathrm{Re}}\sin 2\alpha + a_{22}^{E,\mathrm{Im}}\cos 2\alpha\right)\cos\delta - \left(a_{22}^{M,\mathrm{Re}}\cos 2\alpha - a_{22}^{M,\mathrm{Im}}\sin 2\alpha\right)\sin 2\delta, \\
\Delta\delta \;=\;& -R_1\sin\alpha + R_2\cos\alpha - D_1\cos\alpha\sin\delta - D_2\sin\alpha\sin\delta + D_3\cos\delta + a_{20}^{E}\sin 2\delta \\
-\;& \left(a_{21}^{E,\mathrm{Re}}\cos\alpha - a_{21}^{E,\mathrm{Im}}\sin\alpha\right)\cos 2\delta - \left(a_{21}^{M,\mathrm{Re}}\sin\alpha + a_{21}^{M,\mathrm{Im}}\cos\alpha\right)\sin\delta \\
-\;& \left(a_{22}^{E,\mathrm{Re}}\cos 2\alpha - a_{22}^{E,\mathrm{Im}}\sin 2\alpha\right)\sin 2\delta + 2\left(a_{22}^{M,\mathrm{Re}}\sin 2\alpha + a_{22}^{M,\mathrm{Im}}\cos 2\alpha\right)\cos\delta
\end{aligned}
$$

where R1, R2, R3 are rotation angles around the X, Y, and Z axes of the celestial reference frame, respectively, D1, D2, D3 represent the glide parameters, and $\Delta\alpha$ and $\Delta\delta$ are coordinate differences between the studied and the ICRF2 catalogs. All other parameters are relevant to the quadrupolar deformation. The parameters were fitted by weighted least squares to the coordinate difference of the common sources between the catalogs and the references. The covariance (weight) matrix included the a priori covariance information between the provided estimates of the radio source coordinates. A representation of the rotation and glide parameters is displayed in Fig. 3. The standard deviation and chi-squared of the offsets to the reference before and after removal of the systematics is reported in Table 2. Generally, largest excursion from the ICRF2 show up for the D3 parameters expressing a poleward displacement of the sources. For Australian solutions, both rotation and glide parameters remain unsignificant. Interestingly, the poleward deformation also shows up for the comparison against Gaia but with the reversed sign indicating that the 2016 VLBI catalog deformation lies somewhere between the ICRF2 and Gaia.
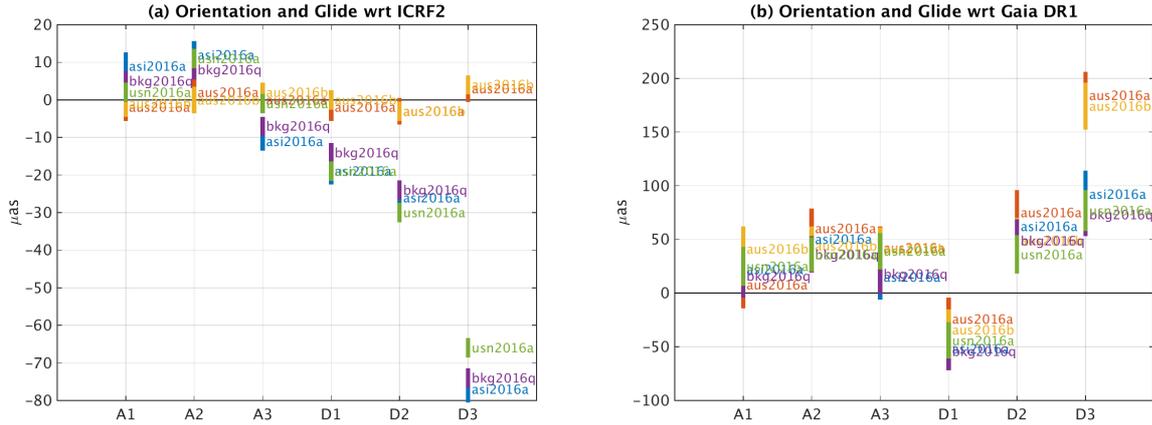
Figure 3. The rotation and glide parameters between the catalogs and the reference that are (Left) the ICRF2 and (Right) Gaia DR1. Unit is microarc second.

3. Zonal errors

In Fig. 4, we plotted the differences in declination between catalogs and the reference averaged in ten bins of declination of equal width between -70° and +70°. The systematics were not removed, so that the differences are direct differences between the catalogs and the reference. Data have been weighted using the total variance coming from the errors in the two compared solutions. Comparison against ICRF2 (panel (a)) revals that the differences are generally increasing in absolute value when going southern except for tha Australian solutions, which is consistent with the estimated rotation and glide parameters (Fig. 3). If one consider that (i) zonal errors in VLBI catalogs can be expected because of the network north-south asymetry and (ii) the Gaia catalog has no zonal error or, at least, smaller than for VLBI, plots of Figs. 3 and 4 can provide insights in how much VLBI catalogs have improved since the ICRF2 from the zonal deformation point of view. Especially, in the (b) panels of the figures, the deformation and declination difference values relevant to Australian solutions are similar to what one would have obtained by comparing the ICRF2 to Gaia. The 2016 ASI, BKG, and USNO solutions appear therefore "closer" to Gaia for D3 and in terms of declination differences.

Table 2. Crude and residual (i.e., after removal of systematics) differences between catalogs and references (ICRF2 and Gaia DR1). Unit is microarc second. Values for right ascension, referred to as RA*, are corrected from the cosine of the declination.

	Differences				Residuals			
	Stdev		Chi2		Stdev		Chi2	
	RA*	Dec	RA*	Dec	RA*	Dec	RA*	Dec
ICRF2								
asi2016a	83	102	0.85	0.91	80	94	0.79	0.78
aus2016a	122	137	0.62	0.57	121	136	0.62	0.57
aus2016b	108	123	0.54	0.51	108	123	0.54	0.51
bkg2016a	89	113	0.44	0.49	87	106	0.42	0.43
usn2016a	96	118	0.47	0.49	93	112	0.44	0.44
Gaia								
asi2016a	363	461	1.88	1.47	357	457	1.82	1.45
aus2016a	537	700	1.59	1.40	532	696	1.57	1.39
aus2016b	519	696	1.59	1.41	516	694	1.57	1.41
bkg2016a	493	627	1.77	1.49	490	624	1.75	1.48
usn2016a	464	570	1.69	1.33	463	567	1.68	1.32
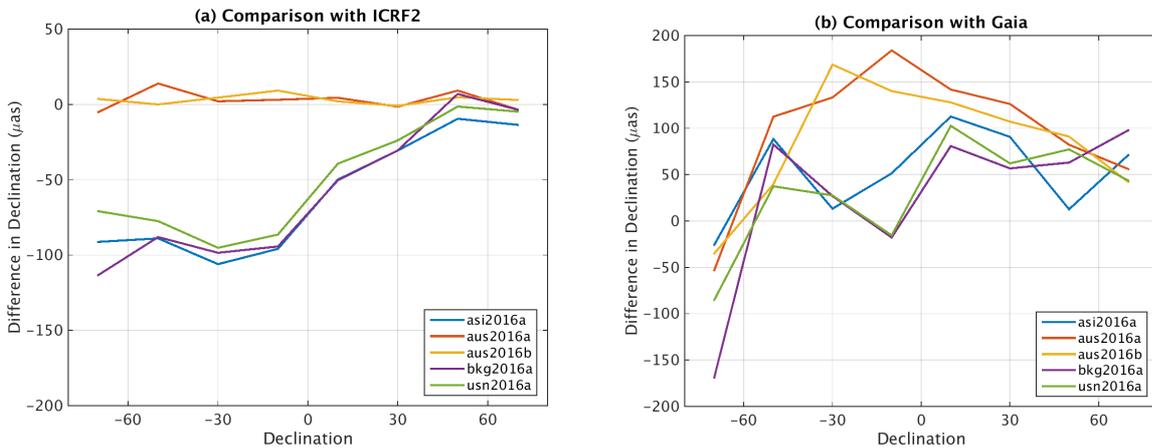
Figure 4. Difference in declination between catalogs and the references binned by interval of declination.

6. References

Fey A, Gordon D, Jacobs C, Ma C, Gaume R, Arias E, Bianco G, Boboltz D, Böckmann S, Bolotin S, et al (2015) The second realization of the international celestial reference frame by very long baseline interferometry. The Astronomical Journal 150(2):58

Mignard F, Klioner S (2012) Analysis of astrometric catalogues with vector spherical harmonics. Astron- omy & Astrophysics 547:A59

Mignard F, Klioner S, Lindegren L, Bastian U, Bombrun, A, Hernandez, J, Hobbs, D, Lammers, U, Michalik, D, Ramos-Lerate, M, Biermann, M, Butkevich, A, Comoretto, G, Joliet, E, Holl, B, Hutton, A, Parsons, P, Steidelmuüller, H, Andrei, A, Bourda, G, Charlot, P (2016) Gaia data release 1 - reference frame and optical properties of icrf sources. Astronomy & Astrophysics 595:A5, DOI 10.1051/ 0004-6361/201629534, URL https://doi.org/10. 1051/0004-6361/201629534